Modeling Flow-Induced Orientation of Fibers Using a New Closure Model

Dilip K. Mandal [1], Andre Benard [1], and Charles A. Petty [2]

[1] *Department of Mechanical Engineering, Michigan State University*
2555 Engineering Building, East Lansing, MI, 48824
[2] *Department of Chemical Engineering and Materials Science, Michigan State University*
2527 Engineering Building, East Lansing, MI 48824
And Corresponding Author's e-mail:benard@egr.msu.edu

SUMMARY: The microstructure and rheology of suspensions can be characterized by using low-order statistical moments of the orientation distribution function. This is illustrated by calculating the orientation dyad and the fiber induced stress for Couette flow between two eccentrically situated cylinders. Other geometries are also considered. Under the conditions studied, the eigenvalues of the orientation dyad remain nonnegative throughout the flow domain. The results are compared with other theories for the microstructure that show unrealizable behavior under the same conditions.

KEYWORDS: *fiber suspensions, fiber orientation, non-Newtonian, closure model, finite elements*.

INTRODUCTION

The properties of short fiber composite are strongly influenced by the orientation of the fibers in the final product. Advani and Tucker [1] discuss the utility of predicting the local microstructure of composites during processing by using low-order moments of the distribution function for the orientation unit vector. This approach, albeit appealing for its low computational cost, unfortunately requires a statistical closure model for the orientation tetrad. In this paper, the microstructure induced by Couette flow between two eccentrically situated cylinders is calculated by using a *fully symmetric quadratic* (FSQ-) closure for the orientation tetrad developed by Petty *et al.*[2]. For comparison, the microstructures predicted by using a *hybrid* closure (see Advani and Tucker [1]) and a *quadratic* closure (see Doi and Edwards [3]) are also presented.

MICROSTRUCTURE THEORY

With $\underline{p}$ defined as a unit vector oriented parallel to the major axis of a rigid fiber, the fraction of fibers having orientation coordinates on the unit sphere in the range $0 \le \theta \le \theta + \Delta\theta$ and $0 \le \phi \le \phi + \Delta\phi$ is given by

$$P\{0 \le \theta \le \theta + \Delta\theta,\ 0 \le \phi \le \phi + \Delta\phi\} = \Psi(\theta, \phi, t)\sin(\theta)\, d\theta\, d\phi \tag{1}$$

where $\Psi(\theta, \phi, t)$ is the orientation distribution function for fibers. For fiber suspensions with an aspect ratio L/d >>1, $\Psi(\theta, \phi, t)$ is governed by Smoluchowski's equation (see Bird *et al.* [4]; Doi and Edwards [3]; Larson [5]):

$$\frac{D\Psi}{Dt} + \frac{\partial}{\partial \underline{p}} \cdot \left[(\underline{p} \cdot \nabla \underline{u} - \underline{p}\,\underline{p}\,\underline{p} : \nabla \underline{u})\Psi \right] = D_R \frac{\partial}{\partial \underline{p}} \cdot \frac{\partial \Psi}{\partial \underline{p}} . \tag{2}$$

A realizable orientation distribution function must satisfy the following normalization condition

$$\int_0^{2\pi} \int_0^{\pi} \Psi(\theta, \phi, t)\sin(\theta)\, d\theta\, d\phi = 1 . \tag{3}$$

In eqn (2), D_R is a rotary diffusion coefficient and has units of 1/time.

Low-order moments of the orientation distribution function are used to characterize the microstructure of fiber suspensions. For example, the second moment, or orientation dyad, is defined as

$$< \underline{p}\,\underline{p} > \equiv \int_0^{2\pi} \int_0^{\pi} \underline{p}\,\underline{p}\, \Psi(\underline{p}, t)\sin(\theta)\, d\theta\, d\phi . \tag{5}$$

An evolution equation for $< \underline{p}\,\underline{p} >$ consistent with eqn (2) is

$$\frac{D < \underline{p}\,\underline{p} >}{Dt} = (\nabla \underline{u})^T \cdot < \underline{p}\,\underline{p} > + < \underline{p}\,\underline{p} > \cdot \nabla \underline{u} - 2 < \underline{p}\,\underline{p}\,\underline{p}\,\underline{p} > : \underline{\underline{S}} - 6 D_R (< \underline{p}\,\underline{p} > - \frac{1}{3}\underline{\underline{I}}) . \tag{6}$$

In the above equation, $\nabla \underline{u}$ is the velocity gradient and $\underline{\underline{S}}$ is the strain rate. It is noteworthy that the orientation tetrad directly impacts the microstructure by directly coupling with the strain rate, $< \underline{p}\,\underline{p}\,\underline{p}\,\underline{p} > : \underline{\underline{S}}$. Solutions to eqn (6) are symmetric and have the required property that $\mathrm{tr} < \underline{p}\,\underline{p} > = 1$ provided that: 1) the closure model for $< \underline{p}\,\underline{p}\,\underline{p}\,\underline{p} > : \underline{\underline{S}}$ is symmetric, and 2) tr ($< \underline{p}\,\underline{p}\,\underline{p}\,\underline{p} > : \underline{\underline{S}}$) reduces to $< \underline{p}\,\underline{p} > : \underline{\underline{S}}$. The three orientation tetrads examined hereinafter have these two features.

A *fully symmetric quadratic* (FSQ-) closure for the orientation tetrad was introduced by Petty *et al.* [2] in order to preserve the six fold symmetry and contraction properties of $<\underline{\underline{pppp}}>$. The closure is defined by the following set of equations:

$$<\underline{pppp}> = (1 - C_2) <\underline{pppp}>_1 + C_2 <\underline{pppp}>_2 \text{ , where} \tag{7}$$

$$<\underline{pppp}>_1 = -\frac{1}{35} S[\underline{\underline{I}}, \underline{\underline{I}}] + \frac{1}{7} S[\underline{\underline{I}}, <\underline{pp}>] \text{, and} \tag{8}$$

$$\begin{aligned} <\underline{pppp}>_2 = {} & \frac{2}{35} <\underline{pp}> : <\underline{pp}> S[\underline{\underline{I}}, \underline{\underline{I}}] \\ & + S[<\underline{pp}><\underline{pp}>, <\underline{pp}><\underline{pp}>] . \\ & - \frac{2}{7} S[\underline{\underline{I}}, <\underline{pp}><\underline{pp}>] \end{aligned} \tag{9}$$

The result of the operation $S[\underline{\underline{A}}, \underline{\underline{B}}]$ yields a fully symmetric tetradic-valued operator formed from the two indicated symmetric dyadic-valued operators. In general, C_2 depends on the eigenvalues of the orientation dyad. At the nematic state (perfectly aligned), C_2 must be equal to 1/3. At the smectic state (i.e., 2D isotropic state), C_2 must be equal to 1/2. For the calculations presented hereinafter, C_2 is approximated as 0.37 for all orientation states.

Other closures for the orientation tetrad include the quadratic closure used by Doi and Edwards [3] for liquid crystalline polymers:

$$<\underline{pppp}> = <\underline{pp}><\underline{pp}>, \tag{11}$$

and the hybrid closure used by Advani and Tucker [1] for suspensions:

$$<\underline{pppp}> = 27 \det(<\underline{pp}>) <\underline{pppp}>_1 + (1 - 27 \det(<\underline{pp}>)) <\underline{pp}><\underline{pp}>. \tag{12}$$

Unlike the *fully symmetric quadratic* (FSQ-) closure defined above, eqns (11) and (12) do not satisfy the six fold symmetry and contraction properties of the exact orientation tetrad. However, they do satisfy the two conditions identified below eqn (6).

The foregoing theory directly influences the rheology of the fiber suspension through an elastic contribution to the deviatoric component of the stress:

$$\underline{\underline{\tau}} = 2\mu \underline{\underline{S}} + k <\underline{pppp}> : \underline{\underline{S}} . \tag{13}$$

In the above equation, μ is the shear viscosity of the continuous phase and the elastic coefficient k, which is proportional to the viscosity, depends on the volume fraction and the aspect ratio of the fibers (Bird *et al.*[4]; Bhave *et al.* [6]). For the calculations presented in this paper, $\mu = 1.5$ N-s/m^2, $k = 3.0$ N-s/m^2, and $\rho = 1260$ kg/m^3.

The velocity and pressure fields are determined by solving the continuity equation,

$$\nabla \cdot \underline{u} = 0 , \tag{14}$$

and the equation of motion:

$$\rho \frac{D\underline{u}}{Dt} = -\nabla P + \nabla \cdot \underline{\underline{\tau}} . \tag{15}$$

Computational Approach

A Petrov-Galerkin finite element method with 496 quadratic elements and 2,108 nodes was used to develop a steady state solution to eqns (6), (14), and (15) with $D_R = 0$ (see Yu and Heinrich [7]). The radius of the larger cylinder R = 100mm and the radius of the smaller cylinder r = 50 mm. The two cylinders have an offset of 25-mm (see Figure 1). A no-slip boundary condition was imposed on the velocity at solid fluid interfaces. The angular velocity of the outer cylinder is $0.336\ \nu/R^2$, where ν is the kinematic viscosity of the fluid. The inner cylinder is stationary. A similar problem was analyzed by Feng and Leal [8] for liquid crystalline polymers by using a quadratic closure for the orientation tetrad.

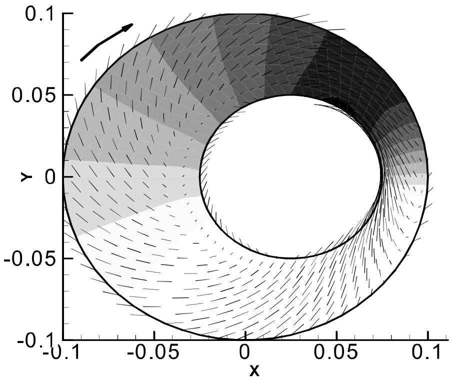

Figure 1 Distribution of the orientation director and the pressure field in the gap between a rotating cylinder and a stationary eccentric cylinder predicted by using the *FSQ-closure* for the orientation tetrad. Shorter director lengths indicate a nearly isotropic microstructure and longer director lengths indicate a highly aligned (nematic-like) microstructure. The darker gray scales identify relatively high-pressure regions; the lighter gray scales identify relatively low-pressure regions. The smallest eigenvalue associated with the director is 1/3 and occurs in regions where the strain rate is small.

A steady state solution was developed by solving an initial value problem with

$$<\underline{p}\underline{p}>_o = \frac{1}{3}\underline{\underline{I}}\,. \qquad (16)$$

Quiescent initial conditions were specified for the velocity and pressure fields. A successive substitution scheme (Picard iteration) with a relaxation factor of 0.5 was used to solve the set of non-linear equations. A first order implicit scheme was used with a time step of approximately $0.05R^2/\nu$. The Reynolds number Re ($\equiv \Omega R^2/\nu$) = 0.336.

The eigenvector associated with the largest eigenvalue of the orientation dyad is defined as the microstructure director $<\underline{N}>$. All the eigenvalues of $<\underline{p}\,\underline{p}>$ are real and satisfy the inequality $0 \le \lambda \le 1$. Models for the orientation dyad that satisfy this feature are realizable. The eigenvectors of the anisotropic component of $<\underline{p}\,\underline{p}>$, defined by

$$\underline{\underline{b}} \equiv <\underline{p}\,\underline{p}> - \frac{1}{3}\underline{\underline{I}}\,, \qquad (17)$$

are the same as the eigenvectors of $<\underline{p}\,\underline{p}>$. The eigenvalues of $\underline{\underline{b}}$ and the eigenvalues of $<\underline{p}\,\underline{p}>$ are related by

$$\beta = \lambda - \frac{1}{3}\,. \qquad (18)$$

Therefore, $\frac{1}{3} \le \lambda_{max} \le 1$ and $0 \le \beta_{max} \le \frac{2}{3}$. The vector field defined by $\underline{n} \equiv \beta_{max} <\underline{N}>$ can be used to characterize the local microstructure of a suspension. For an isotropic microstructure, $\underline{n} = \underline{0}$; for a highly aligned nearly nematic microstructure, $\underline{n} \cong \frac{2}{3} <\underline{N}>$.

RESULTS AND CONCLUSIONS

Figures 1 and 2 show the distribution of the scaled director $\underline{n} \equiv \beta_{max} <\underline{N}>$ for the FSQ-closure, hybrid closure, and the quadratic closure, respectively. The FSQ-closure for the orientation tetrad gives a realizable microstructure whereas the hybrid closure and the quadratic closures produce small regions where the maximum eigenvalue of the orientation dyad is larger than unity, which is an unphysical result.

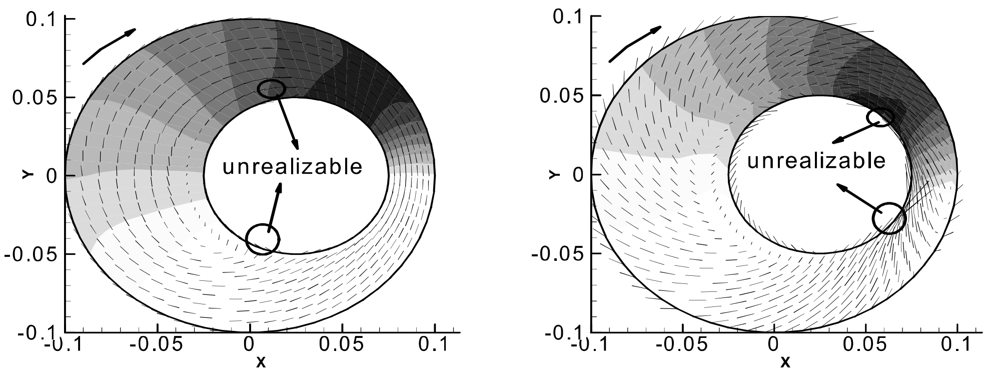

Figure 2. Distribution of the orientation director and the pressure field in the gap between a rotating cylinder and a stationary eccentric cylinder predicted by using the hybrid (left) and the quadratic (right) closures for the orientation tetrad.. The maximum eigenvalue associated with the director for the orientation dyad predict by the hybrid closure is 1.03 and 1.4 for the quadratic closure, which are unphysical. The smallest eigenvalue associated with the director is 1/3 and occurs in regions where the strain rate is small. A small unrealizable region develops in the flow field as indicated in the figures above.

The overall microstructure produced by the FSQ-closure and the quadratic closure are similar (see Figures 1 and 2); however, the hybrid model defined by eqn (12) produced a qualitatively different microstructure for the same complex flow field. The pressure distribution was similar for all three models. A recirculating region close to the small cylinder developed on the large gap side. Note that the fibers are randomly oriented in this region. Outside the circulating region, the fibers tend to orient with the velocity field. The fibers tend to be highly aligned in the small gap region where the strain rate is high.

REFERENCES

[1] Advani, S.G & Tucker, C.L, Closure approximation for three-dimensional structure tensors, Journal of Rheology, 34:367-386, 1990.
[2] Petty, C. A., Parks, S. M. & Shao, S. M., Flow Induced Alignment of Fibers, in Proceedings of *12th International Conference on Composite Materials*, ICCM12/TCA, Paris, July 5-9, 1999.
[3] Doi, M. & Edwards, S. F., *The Theory of Polymer Dynamics*, International Series of Monographs on Physics 73, Oxford University Press, 1998.
[4] Bird, R.B., Armstrong, R.C. & Hassager, O. *Dynamics of Polymeric Liquids*, Volume 2, John Wiley, 1987.
[5] Larson, R. G., *The Structure and Rheology of Complex Fluids*, Oxford University Press,1999.
[6] Bhave, A. V., Menon., R. K., Armstrong, R. C. & Brown, R. A., A Constitutive Equation for Liquid-Crystalline Polymer Solutions, *Journal of Rheology*, 37(3), 413-441,1993.
[7] Yu, C.-C & Heinrich, J.C., Petrov-Galerkin methods for the time dependent convective transport equation, Journal for Numerical Methods in Engineering, 23:883-901, 1986.
[8] Feng, J. & Leal, L.G., Simulating complex flows of liquid-crystalline polymers using the Doi Theory, Journal of Rheology, 41:1317-1335, 1997.